SAND--89-0736C

CONF-890335--13

DE89 009070

STATUS OF THE PBFA-II LIGHT ION BEAM FUSION PROGRAM

J. P. Quintenz, J. E. Bailey, K. W. Bieg, D. D. Bloomquist, D. L. Cook, J. T. Crow, R. S. Coats, M. S. Derzon, M. P. Desjarlais, P. L. Dreike, R. A. Gerber, T. W. Hussey, D. J. Johnson, W. A. Johnson, R. P. Kensek, G. W. Kuswa, J. R. Lee, R. J. Leeper, T. R. Lockner, J. E. Maenchen, D. H. McDaniel, P. F. McKay, T. A. Mehlhorn, C. W. Mendel, Jr., L. P. Mix, E. L. Neau, C. L. Olson, T. D. Pointon, A. L. Pregenzer, T. J. Renk, G. E. Rochau, S. E. Rosenthal, C. L. Ruiz, L. X. Schneider, S. A. Slutz, R. W. Stinnett, W. A. Stygar, M. A. Sweeney, G. C. Tisone, B. N. Turman, J. P. VanDevender, and J. R. Woodworth

Sandia National Laboratories
P. O. Box 5800
Albuquerque, New Mexico 87185

Abstract

PBFA II is the first pulsed power accelerator designed and built specifically to produce light ions for driving targets in Sandia National Laboratories' inertial confinement fusion program. Recent progress in ion beam generation and focusing has been excellent. Record ion beam intensities have been obtained. Development of an extensive array of diagnostics and advances in the theory of ion diodes have had a major impact on this progress. A summary of recent progress and the present status of the PBFA-II light ion beam fusion program is given.

Introduction

The Particle Beam Fusion Accelerator II (PBFA II) is being developed at Sandia National Laboratories to provide a power source for driving Inertial Confinement Fusion (ICF) targets.[1-2] Light ion beams offer an attractive driver for ICF because these beams can be efficiently generated at a cost that is low relative to other drivers being considered for ICF. The requirements for achieving thermonuclear ignition with ion driven inertial confinement are very demanding. With current target designs, the ion beam must deposit greater than 1 million joules (MJ) of energy in a target ~ 1 cm in diameter on a time scale of a few tens of nanoseconds (ns) to compress the target fuel, a mixture of deuterium and tritium (DT), to a density of approximately 1000 times that of liquid DT. This will require focusing of the ion beam to a peak intensity of ~ 50-100 terawatts (TW) per square centimeter.[3]

PBFA II is the first pulsed power accelerator specifically designed to produce intense light ion beams for ICF research.[4] It was first fired in December 1985 and since that time significant progress has been made in accelerator performance, reliability, and shot rate.[5] The ion beam is produced near the center of PBFA II in an ion diode where electromagnetic energy is converted into beam kinetic energy. Since the first experiments with magnetically insulated ion diodes in the late 1970's,[6-8] progress in ion beam generation and focusing in these devices has been substantial.[9-14] This progress has been aided by advances in the theory of magnetically insulated ion diodes and by an expanded and improved array of intense beam diagnostics. PBFA II ion beam production is approaching levels where significant target experiments can be performed.

The PBFA-II Accelerator

PBFA II is shown in an artist's cutaway drawing in Fig. 1. It consists of 36 Marx generators storing a total of 13 MJ of energy at full charge. Each of the 36 modules in PBFA II delivers energy from an oil dielectric energy storage section (370 kJ, 6 MV, 1 μs), through a water dielectric pulse forming section (80 kJ, 3.2 MV, 55 ns) to a common vacuum insulator stack with diameter of 3.6 m. A research effort is underway to improve the efficiency of the transformers in the water section. The goal is to increase the 80 kJ/module forward going energy to 120 kJ/module.[15] The energy from each module (in the form of electromagnetic energy and magnetically insulated electron flow) is combined in a parallel-series combination in the vacuum section to provide a 12 MV pulse at a radius of approximately 50 cm. The pulse then flows toward the ion diode in a vacuum biconic feed. The stringent requirements on the pulse duration and symmetry at the target located in the center of the accelerator force a high degree of synchronization of the 36 individual modules in PBFA II. The required level of synchrony and symmetry has been achieved, and first-to-last-module timing spreads of 15 ns and standard deviations of 3.5 ns are routinely produced.[16]

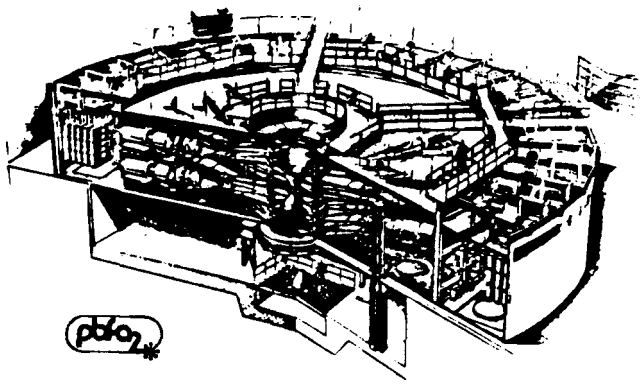

Figure 1. Sectioned line drawing of PBFA II.

In order to reach the goal of a 30 MV, 100 TW, 15 ns power pulse at the ion diode, PBFA II was designed to use the inductance of the vacuum power feed as an energy store. This in turn requires a fast opening switch (a plasma opening switch on PBFA II) to deliver the energy to the ion diode on this time scale. Circuit simulations indicate that a switch whose impedance rises from zero to forty ohms in ten nanoseconds will meet this requirement. Figure 2 shows the biconic feed, plasma opening switch region, ion diode, and diagnostic layout in PBFA II. During the past year, three plasma opening switch configurations have been tested at the half-energy level on PBFA II into 5-ohm electron-beam diodes.[17] These configurations all make use of magnetic fields to control the movement of the switch plasma in the vacuum power feed. The first configuration used an azimuthally segmented switch in which self-magnetic fields help to contain the plasma. The second configuration, called a magnetically injected plasma switch, used an externally applied magnetic field to guide the plasma into the vacuum power feed.[18] This field also sets the opening current level of the switch: the switch begins to open when the self B_θ magnetic field exerts a force that overcomes the applied B_z and B_r field and plasma inertia. The third approach adds a self-energized, fast-rising B_z field coil to enhance the magnetic pressure that drives the switch open.[19] These latter two switch configurations are being pursued

* This work supported by the U.S. Department of Energy under Contract No. DE-AC04-76-DP00789.

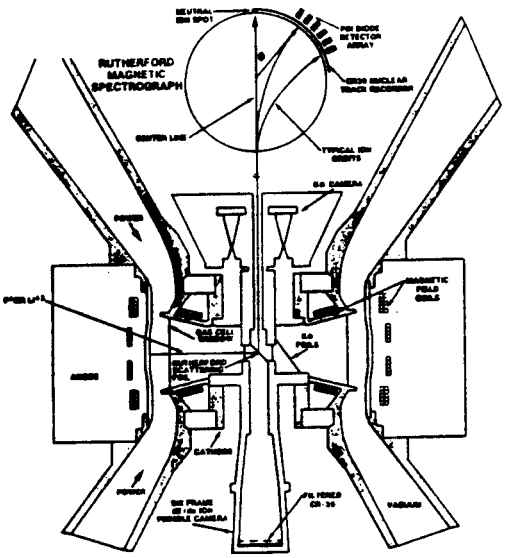

Figure 2. PBFA-II biconic power feed and ion diode, including the ion beam diagnostic layout. The plasma opening switch is located in the power feed above and below the diode.

as we scale up to full power operation on the accelerator. Figure 3 shows the experimentally measured upstream and downstream currents and the circuit model currents and switch voltage for the magnetically injected plasma opening switch. The agreement between the experimental and calculated waveshapes is excellent and comparison of the upstream and downstream experimental currents indicates that the switch couples efficiently to a 5-ohm electron-beam load. Nevertheless, the difference between anode and cathode currents at the load suggests that performance can be further enhanced if power flow losses from electron flow to the anode are reduced.[20] These electrons are actually launched in the plasma opening switch region.

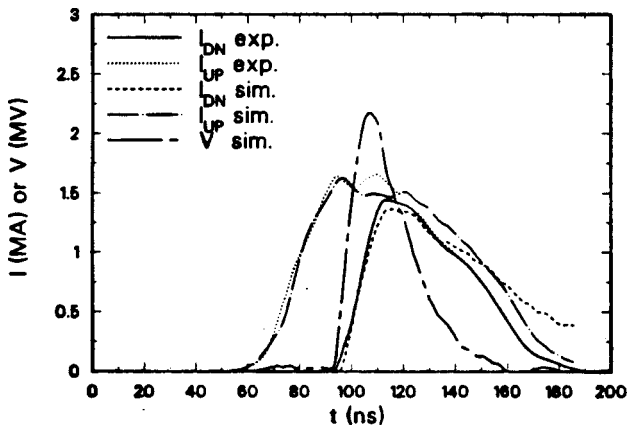

Figure 3. Comparison of measured POS currents with those predicted by circuit simulation.

At half energy (6.5 MJ stored in the Marx generators), all three of these switch configurations demonstrated fast opening times that would give 30 MV at the ion diode at the full upgraded energy level. However, more research will be required to maintain this opening time into an ion diode at 30 MV, an energy level for which the losses from the electron flow launched in the switch region must be reduced. Moreover, so far, coupling of an ion diode to these switches has only been tested for the segmented configuration. (This switch sharpened the risetime of the ion diode current by a factor of two.) The desire to have a rugged switch which fully removes the plasma from the vacuum power feed and offers operational ease of setting the switch opening current level has driven our selection of a plasma opening switch that uses an externally applied magnetic field.

Ion Diode Research

Our learning rate in ion diode research is directly related to the shot rate that we are able to obtain on our accelerators. We have made substantial progress in fielding fully diagnosed ion diode experiments on PBFA II. We have progressed from one full energy shot every three weeks, obtained during the accelerator's first year or "shakedown" phase, to one shot each day at the 3/4 energy level. This higher shot rate has been made possible by the redesign of some accelerator components that were susceptible to breakage and by improvements in operational procedures. While these improvements were being made, the diode experimental team has progressed through a sequence of experiments at the 1/4, 1/2 and recently, 3/4 energy levels at the new high shot rate. We are now near the point where full energy shots at this rate will be practical.

In a high power diode, the electric field stresses (> 1 MV/cm) and power levels (> 1 TW) are sufficient to generate a plasma at the surface of the diode negative electrode (the cathode). The cathode then becomes a space-charge-limited emitter of electrons which are accelerated toward the positive electrode (the anode). A passive ion source (such as a dielectric flashover anode) creates an anode plasma after some time delay and the anode thus becomes a space-charge-limited emitter of ions. In a diode designed to accelerate ions, electron currents constitute an inefficiency and must be minimized. In an applied-B ion diode, an external transverse magnetic field is applied in the region between the anode and cathode to inhibit the crossing of electrons from cathode to anode. The electrons flow in a sheath along a magnetic flux surface and drift in the E X B (azimuthal) direction. This sheath establishes an equipotential surface called a "virtual cathode." The ions are accelerated in the gap between the anode plasma and this virtual cathode and, being more massive, easily cross the magnetic field. In this manner, diodes have been developed that produce ion currents which are in excess of 90% of the total diode current.

A major cause of inefficiency in these diodes has been the falling diode impedance during the accelerator power pulse. Typically, the voltage pulse on the diode leads the diode current by 5-10 ns and the voltage falls continuously as the ion current rises. A falling impedance diode couples less energy into the ion beam than would a constant or rising impedance diode. An increasing current, together with a decreasing ion kinetic energy, exacerbates the problem of beam focusing because the beam focus moves in time due to self-magnetic field focusing. Careful analysis of experimental data from several accelerators yielded an empirical scaling law for the diode impedance.[21] This scaling law suggested the existence of a limiting voltage at which the ion current diverges. An analytic theory[22] of applied-B ion diodes has recently been developed that explains much of the behavior of these diodes, including the empirical scaling. This theory has been used to predict the voltage-current characteristics of these diodes, and, when combined with a simple circuit model of the accelerator, it has been used to calculate diode operating points. The theory has been successfully used to calculate the operating point at peak power of diodes on several different accelerators, as

shown in Fig. 4. A key element of the theory is the determination of the self-consistent motion of the virtual cathode during the diode power pulse.[23] The virtual cathode moves during the pulse because of the diamagnetic field produced by the azimuthal component of the electron current. A relation for the virtual cathode position follows from solving Maxwell's equations in the diode and recognizing that magnetic flux is conserved in two regions: between the anode and the virtual cathode, and between the virtual cathode and the gas-filled beam transport cell. A very important result from the theory is the realization that there is a critical voltage, V_*, at which the ion current diverges. This is a limiting voltage and can be shown to be $V_* \sim \alpha c B_0 d$, where B_0 is the applied magnetic field, d is the anode-cathode gap, and α is between 0.6 and 0.75 depending upon the electron distribution across the gap. Theory and experiments are in excellent agreement for $\alpha = 0.6$, suggesting a constant electron density between the cathode and anode. This is consistent with recent experimental measurements of the electrostatic potential in ion diodes.[24]

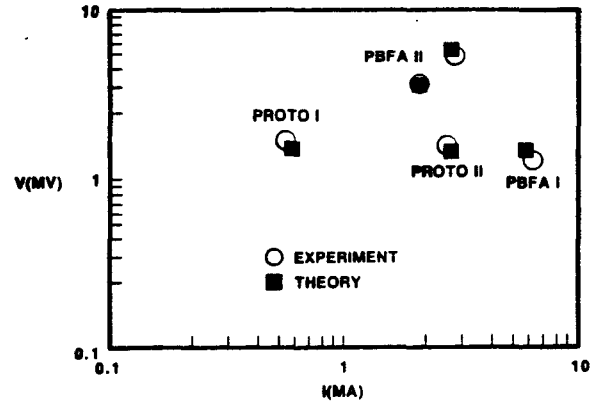

Figure 4. Comparison of ion diode operating points on several accelerators with theoretically predicted values.

In addition to predicting diode operating points at peak power correctly, the analytic diode theory has also given insight into a possible cause of the falling diode impedance.[23] Since the virtual cathode location, and hence the effective anode-cathode gap, depends upon the amount of flux between the anode and the virtual cathode, a decrease in flux between the virtual cathode and the surface of the anode plasma would produce a configuration in which the ion current is more highly enhanced over the space-charge-limited value determined by geometry. Earlier research has raised the possibility that charge exchange processes can play a significant role in these devices.[25] Recent theoretical work has illuminated the role of charge exchange processes in determining diode impedance.[26,27] A falling impedance time history that matches experimental results can be obtained using reasonable neutral densities (10^{18} cm^{-3}) and layer thicknesses (1 mm).[28] Charge exchange interactions can also lead to a spread in the energy of the beam ions. An obvious solution to this problem is to reduce the neutral population in the ion source region.

Development of an ion source that produces a pure (> 90%) Li^+ beam with a low neutral fraction is a high priority research effort in our program. Two candidate lithium sources are the BOLVAPS/LIBORS[29] ion source and the EHD ion source.[30] In the BOLVAPS/LIBORS source, a lithium-bearing thin film is ohmically heated rapidly to produce a lithium vapor that is subsequently ionized by a laser pulse. Small scale tests of this concept have produced Li^+ plasmas with low neutral content. The electrohydrodynamically (EHD) driven liquid metal ion source produces lithium ions by field emission from closely spaced cusps created when a layer of liquid lithium is subjected to the diode's strong electric field. The cusps form as the result of an electrohydrodynamic instability. This will be the first large-area EHD source to be developed. EHD point sources are commonly used to produce high-brightness ion beams for surface analysis, lithography, and microfabrication. Both of these sources will be tested on PBFA II this year.

Focusing the ion beam in an applied-B ion diode requires control of several competing mechanisms. The beam focusing problem can be divided into two orthogonal planes: vertical (r,z), and horizontal (r,θ). In the vertical direction the beam is deflected by electrostatic forces in the A-K gap, by self-magnetic B_θ fields wherever the beam current is unneutralized, and by applied-magnetic fields in the neighborhood of the cathode field coils. Horizontal focusing errors can result from any effect that causes the beam ions to arrive near the diode axis with non-zero canonical angular momentum. These effects can include applied-magnetic field stream function errors at the anode or gas cell (where nonprotonic ions can be stripped of electrons and undergo a discrete change in canonical angular momentum) and time dependent changes in the stream function at the ion source such as the charge exchange mechanism described above. Both vertical and horizontal errors can be introduced by ion source nonuniformities, fluctuations due to instabilities in the acceleration and transport regions of the diode, scattering and energy loss in the gas cell, mechanical misalignment, and other effects. Many of these effects have been investigated with computer simulation codes. We are in the process of evaluating the relative importance of each cause of beam focusing error.

Some of these errors can be reduced by going to higher ion mass-to-charge ratios and by improving the ion source characteristics. While we are actively pursuing lithium ion sources, we are conducting most of our beam physics experiments with flashover ion sources that produce a mixed species beam of protons, carbon and smaller amounts of heavier ions. In these experiments, all ions except the protons are stopped by the 2-μm thick mylar gas cell membrane. Focusing experiments are done using the proton portion of the beam, which constitutes approximately 50% of the beam current. Recently, proton beams have been focused on PBFA II to spot diameters of < 5.5 mm with a peak intensity of up to 3.8 (+0.7, -0.8) TW/cm^2. On other shots, total proton energy impinging on a 1.0 cm radius target region has been measured to be up to 140 kJ. These high intensities have been obtained by narrowing the anode emission height, thereby both reducing the applied-B field bending of the beam and improving the ion source uniformity, and by shaping the anode to compensate for steering errors that are identified in experiments where a shadowbox technique was used to image the ion vectors.[31]

Beam Diagnostics

A particular difficulty in the PBFA-II ion beam experimental program has been the development of a diagnostic package for adequately measuring the parameters of the intense ion beams produced in these diodes. The difficulty arises from the fact that the ion beams are nearly 100% space-charge and current neutralized. Also, electron losses in the diode produce hard (several MeV) x-ray bremsstrahlung backgrounds of some 10^9-10^{10} rads/sec, and access is limited by the diode and accelerator geometries. In addition, as the beam converges toward the axis, the intensity is so great that usual detectors saturate or fail. We have overcome these problems by using several different diagnostics that are robust in this challenging environment.[32] An x-ray pinhole camera system provides data on the ion fluence near the diode axis (r = 3.8 cm) by imaging K_α x-rays produced when protons or lithium ions strike thick

aluminum or titanium conic targets.[33] A six-frame energy-resolving ion pinhole camera records two-dimensional energy density profiles of the ion beam as a function of ion energy.[34] Ions that strike an on-axis gold Rutherford scattering foil elastically scatter through six pinholes onto separate areas of a sheet of CR-39 nuclear track recording plastic. Each area is covered by an aluminum range filter of varying thickness and records an image with a different lower bound on the ion energy. Ion track densities on the CR-39 are measured with an automated nuclear track counting system.[34] Another imaging diagnostic being developed for PBFA II is a time-resolved ion pinhole camera consisting of an array of PIN diodes viewing ions through holes drilled in the CR-39 in the ion pinhole camera described above. This diagnostic can produce a "movie" of the ion beam on target.[9,32]

In addition to the imaging diagnostics, particle spectrograph and nuclear activation diagnostics have been developed to provide additional beam information. A Rutherford magnetic spectrograph provides time-integrated and time-resolved ion energy spectra, ion species data, and full time-resolved analysis of the ion current density, power density, and mean energy.[35] A Thomson parabola spectrograph is the primary diagnostic for beam composition.[36] Indirect nuclear activation is used to provide information about the total number of ions in the beam.[32] In these diagnostics, proton or lithium beams strike thick targets, which in turn emit high-energy gamma rays or neutrons that then strike remotely located activation targets (typically copper or praseodymium). By measuring the half-life activity of the activated elements, the total number of ions in the beam can be deduced, given V(t) information from the magnetic spectrometer.

As described above, it is becoming more and more important to understand the physics of the anode plasmas in these diodes. One diagnostic technique with considerable promise in this area is visible spectroscopy. The potential of this technique has been demonstrated on a small accelerator by Maron et al.[37] Measurements included anode plasma thickness, uniformity, composition, density and temperature. In addition, E and B fields and ion velocity vectors have been measured. To adapt these methods to PBFA II, several problems must be solved. The first problem is that any collecting optics subjected to the bremsstrahlung background generate Cerenkov light that interferes with the signal. A series of measurements to assess the magnitude of this problem for fiber-optic systems has been performed and we have identified configurations with an acceptable signal-to-noise ratio. The expense of operating a large machine like PBFA II makes it essential to collect data over a large spectral range with both space- and time-resolution on a single shot. To address this problem, a visible and UV spectrograph have been coupled to two streak cameras.[38] Time-resolved spectra from the PBFA-II anode plasma have been obtained with these instruments and the results are being analyzed.

The amount of data gathered on each shot has increased in direct proportion to the number of diagnostics being fielded. With so much data to analyze from each shot and with the increased shot rate, the need for automated data reduction and analysis is paramount. Several new computer programs have been written, greatly improving our data reduction capabilities.[39] We have also written a computer code to forward-predict ion beam transport and diagnostic response.[40] This code can study the effects of net canonical angular momentum, charge exchange, magnetic field configurations, and varying anode heights and shapes on the ion beam transport and focusing. For example, we have used this code to gain an understanding of solenoidal focusing by the applied magnetic field and have shown that the anode must be increasingly convex as a function of height to compensate for this effect. We find good agreement in the energy transported to the axis between our simulations and experiment. This code has also been extremely useful in designing new diagnostics and interpreting diagnostic data on focusing.

Conclusions

An analytic theory of applied-B ion diodes has been developed that correctly predicts the diode operating points at peak power, and there is agreement between simulations and experiment for the ion beam transport to the diode axis. The anode plasma has been identified as an area for study to improve the ion beam focusing and diode impedance behavior further. An extensive array of ion beam diagnostics has been developed and proven to operate well in the harsh x-ray environment of PBFA II. Work on interpreting data from these diagnostics has provided insights into the physics of beam generation and transport and has stimulated advances in both analytic and calculational modeling of these processes. Three plasma opening switch configurations have been identified and tested. These switches have produced fast impedance risetimes into electron-beam loads and research is in progress to extend these results to ion diode loads at 30 MV.

During the past 18 months, we have demonstrated efficient ion beam generation and achieved a focal spot diameter of <5.5 mm at 3/4 energy. The peak proton power density achieved on PBFA II has risen from ~ 0.3 TW/cm^2 to ~ 3.8 (+0.7, -0.8) TW/cm^2 and the total proton energy on a 1.0 cm radius target has increased from 30 kJ to 140 kJ. At these power and energy levels, we can begin to do interesting target experiments. Progress has been rapid in accelerator timing synchronization and reliability, plasma opening switch operation and theory, and advances in the theory and operation of ion diodes and in intense beam diagnostics. The promise of developing lithium ion sources gives us confidence that our goal of 1 MJ of 30 MeV lithium ions focused to 50-100 TW/cm^2 can be achieved on PBFA II.

References

1. J. P. VanDevender and D. L. Cook, *Science*, 232, 831 (1986).
2. D. L. Cook, et al., *Plasma Phys. and Controlled Fusion*, 28, 1921 (1986).
3. J. D. Lindl and J. W-K. Mark, *Lasers and Particle Beams*, 3, 37 (1985).
4. B. N. Turman, et al., *Conf. Record, 5th IEEE Pulsed Power Conf.*, p.155 (1985).
5. D. L. Cook, et al., *Conf. Record, 7th Int'l. Conf. on High-Power Particle Beams*, p.35 (1988).
6. R. N. Sudan and R. V. Lovelace, *Phys. Rev. Lett.*, 31, 1174 (1973).
7. S. Humphries, Jr., J. J. Lee and R. N. Sudan, *J. Appl. Phys.*, 46, 187 (1975).
8. P. L. Dreike, C. Eichenberger, S. Humphries, Jr., and R. N. Sudan, *J. Appl. Phys.*, 47, 85 (1977).
9. D. J. Johnson, et al., *J. Appl. Phys.*, 58, 12 (1985).
10. P. L. Dreike, et al., *J. Appl. Phys.*, 60, 878 (1986).
11. J. E. Maenchen, et al., *Proc. 6th Int. Conf. on High-Power Electron and Ion Beams*, Kobe, Japan, June 9-13, 1986.
12. S. Humphries, Jr., *Nucl. Fusion*, 20, 1549 (1980).

13. C. L. Olson, *J. Fusion Energy*, 1, 309 (1982).

14. J. E. Maenchen, et al., *J. Appl. Phys.*, 65, 448 (1989).

15. L. X. Schneider, E. L. Neau, and W. A. Johnson, *Proc. 7th IEEE Pulsed Power Conference*, Monterey, California, June 11-14, 1989 (to be published).

16. J. M. Wilson and G. L. Donovan, *Conf. Record, 6th IEEE Pulsed Power Conference*, p.361 (1987).

17. G. E. Rochau, *Bull. Am. Phys. Soc.*, 33, 2040 (1988).

18. C. W. Mendel, Jr., *Bull. Am. Phys. Soc.*, 31, 1412 (1986).

19. C. W. Mendel, Jr. et al., *Conf. Record, 15th IEEE Conf. on Plasma Sci.*, p.128 (1988).

20. C. W. Mendel, Jr. et al., *Proc. Intl. Workshop on Phys. and Tech. of High Power Opening Switches*, Novosibirsk, USSR, July 8-9, 1989 (to be published).

21. P. A. Miller, *J. Appl. Phys.*, 57, 1473 (1985).

22. M. P. Desjarlais, *Phys. Rev. Lett.*, 59, 2295 (1987).

23. M. P. Desjarlais, submitted to *Phys. Fluids*.

24. M. D. Coleman, Ph.D. Thesis, Cornell University, 1989.

25. D. S. Prono, et al., *J. Appl. Phys.*, 52, 3004 (1981).

26. T. D. Pointon, submitted to *J. Appl. Phys.*

27. M. P. Desjarlais, submitted to *J. Appl. Phys.*

28. M. P. Desjarlais, *Bull. Am. Phys. Soc.*, 33, 2087 (1988).

29. P. L. Dreike and G. C. Tisone, *J. Appl. Phys.*, 59, 371 (1986).

30. A. L. Pregenzer, *J. Appl. Phys.*, 58, 4509 (1985).

31. D. J. Johnson and T. L. Lockner, private communication.

32. R. J. Leeper, et al., *Rev. Sci. Instrum.*, 59, 1860 (1988).

33. J. Maenchen, et al., *Rev. Sci. Instrum.*, 59, 1706 (1988).

34. W. A. Stygar, et al., *Rev. Sci. Instrum.*, 59, 1703 (1988).

35. R. J. Leeper, et al., *Rev. Sci. Instrum.*, 59, 1700 (1988).

36. C. L. Ruiz, et al., *Conf. Record, 15th IEEE Conf. on Plasma Sci.*, p.55 (1988).

37. Y. Maron, M. D. Coleman, D. A. Hammer, and H. S. Peng, *Phys. Rev. A*, 36, 2818 (1987).

38. J. Bailey, K. W. Bieg, M. J. Hurst, R. L. Morrison, and G. C. Tisone, *Rev. Sci. Instrum.*, 59, 1485 (1988).

39. T. A. Mehlhorn, et al., *Rev. Sci. Instrum.*, 59, 1709 (1988).

40. J. P. Quintenz, et al., *Bull. Am. Phys. Soc.*, 30, 1603 (1985).